Cardiovascular Research (2016) **111**, 287–294
doi:10.1093/cvr/cvw093

Elevated local [Ca^{2+}] and CaMKII promote spontaneous Ca^{2+} release in ankyrin-B-deficient hearts

Iuliana Popescu[1], Samuel Galice[2], Peter J. Mohler[3,4,5], and Sanda Despa[1]*

[1]Department of Pharmacology and Nutritional Sciences, University of Kentucky, 900 S Limestone, Lexington, KY 40536, USA; [2]Department of Pharmacology, University of California Davis, Davis, CA 95616, USA; [3]The Dorothy M. Davis Heart and Lung Research Institute, The Ohio State University Wexner Medical Center, Columbus, OH 43210, USA; [4]Department of Physiology and Cell Biology, The Ohio State University Wexner Medical Center, Columbus, OH 43210, USA; and [5]Department of Internal Medicine, The Ohio State University Wexner Medical Center, Columbus, OH 43210, USA

Received 8 December 2015; revised 15 April 2016; accepted 27 April 2016; online publish-ahead-of-print 30 April 2016

Time for primary review: 44 days

Aims Loss-of-function mutations in the cytoskeletal protein ankyrin-B (AnkB) cause ventricular tachyarrhythmias in humans. Previously, we found that a larger fraction of the sarcoplasmic reticulum (SR) Ca^{2+} leak occurs through Ca^{2+} sparks in AnkB-deficient ($AnkB^{+/-}$) mice, which may contribute to arrhythmogenicity via Ca^{2+} waves. Here, we investigated the mechanisms responsible for increased Ca^{2+} spark frequency in $AnkB^{+/-}$ hearts.

Methods and results Using immunoblots and phospho-specific antibodies, we found that phosphorylation of ryanodine receptors (RyRs) by CaMKII is enhanced in $AnkB^{+/-}$ hearts. In contrast, the PKA-mediated RyR phosphorylation was comparable in $AnkB^{+/-}$ and wild-type (WT) mice. CaMKII inhibition greatly reduced Ca^{2+} spark frequency in myocytes from $AnkB^{+/-}$ mice but had little effect in the WT. Global activities of the major phosphatases PP1 and PP2A were similar in $AnkB^{+/-}$ and WT hearts, while CaMKII autophosphorylation, a marker of CaMKII activation, was increased in $AnkB^{+/-}$ hearts. Thus, CaMKII-dependent RyR hyperphosphorylation in $AnkB^{+/-}$ hearts is caused by augmented CaMKII activity. Intriguingly, CaMKII activation is limited to the sarcolemma–SR junctions since non-junctional CaMKII targets (phospholamban, HDAC4) are not hyperphosphorylated in $AnkB^{+/-}$ myocytes. This local CaMKII activation may be the consequence of elevated [Ca^{2+}] in the junctional cleft caused by reduced Na^+/Ca^{2+} exchange activity. Indeed, using the RyR-targeted Ca^{2+} sensor GCaMP2.2-FBKP12.6, we found that local junctional [Ca^{2+}] is significantly elevated in $AnkB^{+/-}$ myocytes.

Conclusions The increased incidence of pro-arrhythmogenic Ca^{2+} sparks and waves in $AnkB^{+/-}$ hearts is due to enhanced CaMKII-mediated RyR phosphorylation, which is caused by higher junctional [Ca^{2+}] and consequent local CaMKII activation.

Keywords Ankyrin-B • Ca^{2+} sparks • CaMKII • Junctions • Local Ca^{2+} concentration

1. Introduction

Ankyrin-B (AnkB) is an adaptor protein that targets and tethers to the cytoskeleton select membrane proteins, including the Na^+/Ca^{2+} exchanger (NCX),[1–6] the main route for Ca^{2+} extrusion in cardiac myocytes, and the Na^+/K^+ pump (NKA).[1–3,6,7] Loss-of-function mutations in AnkB cause a complex arrhythmogenic phenotype in humans that may include bradycardia, atrial fibrillation, conduction defects, long QT syndrome, and ventricular arrhythmias.[1–3,8–10] Several AnkB variants (including E1425G, V1516D, E1813K, L1622I, and R1788W) are associated with stress-induced ventricular tachyarrhythmias and sudden cardiac death.[1–3,8] However, the mechanisms that link deficient AnkB function to altered electrical signalling in the ventricle are largely unknown.

Spontaneous sarcoplasmic reticulum (SR) Ca^{2+} release during diastole, or SR Ca^{2+} leak, can cause Ca^{2+} waves that activate the Na^+/Ca^{2+} exchanger and thus generate an inward current. This current depolarizes the membrane and, if large enough, triggers a spontaneous action potential.[11] When such depolarizations arise simultaneously in a large number of neighbouring myocytes, they cause spontaneous excitation of the entire heart and may trigger ventricular tachyarrhythmias or fibrillation.

SR Ca^{2+} leak is mediated by ryanodine receptors (RyRs) and occurs either in the form of Ca^{2+} sparks, when multiple (6–20) RyRs within a

* Corresponding author. Tel: +1 859 218 3827, E-mail: s.despa@uky.edu

SR–sarcolemma junction are activated, or as smaller, invisible, events.[12–14] Using mice heterozygous for a null mutation in AnkB (AnkB$^{+/-}$ mice), we previously found that AnkB deficiency leads to more frequent pro-arrhythmogenic Ca^{2+} sparks and waves during diastole.[15] Despite higher Ca^{2+} spark frequency, the total SR Ca^{2+} leak was similar in myocytes from AnkB$^{+/-}$ and wild-type (WT) mice.[15] These results suggest that reduced AnkB function modifies the RyR gating to favour large Ca^{2+} release events (i.e. sparks) at the expense of smaller, non-spark releases. Notably, RyR open probability is augmented in AnkB$^{+/-}$ vs. WT myocytes.[16] We further found that membrane permeabilization with saponin equalizes Ca^{2+} spark frequency in AnkB$^{+/-}$ and WT myocytes,[15] which suggests that decreased AnkB function does not produce major changes in RyR expression and cluster organization. On the basis of these data, we concluded that the more coordinated RyR openings in AnkB$^{+/-}$ myocytes are likely an indirect effect of AnkB reduction, mediated by altered RyR regulation at the cytosolic side.[15]

The RyR open probability, and thus Ca^{2+} spark frequency, is increased by several post-translational modifications of RyRs as well as by direct Ca^{2+} sensitization. While we found that diastolic $[Ca^{2+}]_i$ is similar in myocytes from AnkB$^{+/-}$ and WT mice,[15] RyRs respond to the local Ca^{2+} level in the junctional cleft ($[Ca^{2+}]_{Cleft}$), which is generally different from $[Ca^{2+}]_i$ in bulk cytosol.[17–19] Here, we combine the assessment of RyR post-translational modifications, kinase and phosphatase activity assays, and direct measurements of $[Ca^{2+}]_{Cleft}$ to uncover the mechanisms that link deficient AnkB function to a higher frequency of pro-arrhythmogenic Ca^{2+} sparks and waves.

2. Methods

Detailed methods are included in the Supplementary material online.

2.1 Ventricular myocyte isolation

All animal experiments conform to the NIH guide for the care and use of laboratory animals and were approved by the Institutional Animal Care and Use Committee at University of Kentucky or the Ohio State University. Single ventricular myocytes were enzymatically isolated from hearts of mice heterozygous for AnkB null allele (AnkB$^{+/-}$) and WT littermates as previously described.[15] Briefly, mice were anaesthetized with 3–5% isoflurane and hearts were excised quickly, mounted on a gravity-driven Langendorff perfusion apparatus and perfused with 1 mg/mL collagenase. When the heart became flaccid (11–15 min), the tissue was cut into small pieces, dispersed, and filtered, and the myocyte suspension was rinsed several times. A total of 20 AnkB$^{+/-}$ and 20 WT mice were used for this study. All experiments were done at room temperature (23–25°C).

2.2 Ca^{2+} spark measurements in intact cardiac myocyte

Fluo-4-loaded myocytes were imaged in line-scan mode with a laser-scanning confocal microscope. Myocytes were perfused with 1 mmol/L Ca^{2+} Tyrode's solution and stimulated at various pacing frequencies (0.5, 1, or 2 Hz) until Ca^{2+} transients reached steady state. Stimulation was then stopped and spontaneous Ca^{2+} sparks were recorded in a $0Na^{+}$/$0Ca^{2+}$ Tyrode's solution. Finally, the SR Ca^{2+} content was assessed from the amplitude of the Ca^{2+} transient generated by rapid application of 10 mmol/L caffeine. Ca^{2+} sparks were detected, counted, and characterized using SparkMaster.[20]

2.3 Immunoblot

Proteins from left ventricle homogenates were separated by SDS–PAGE electrophoresis and transferred on PVDF membranes, which were then blocked and probed with primary antibodies against total RyR2 (Abcam, San Francisco, CA, USA), phospho(Ser2814)-RyR2, phospho(Ser2808)-RyR2, total phospholamban (PLB), phospho(Thr17)-specific PLB (Badrilla, Leeds, UK), total CaMKIIδ (Santa Cruz, Dallas, TX, USA), phospho(Thr286)-CaMKII (Abcam), oxidized CaMKII (ox-CaMKII(Met281/2); Genetex, Irvine, CA, USA), total HDAC4 (H-92, Santa Cruz), and phospho(Ser632)-HDAC4 (Abcam). Equal loading was verified by re-probing with anti-GAPDH. Bands were detected by chemiluminescence. Protein band intensity was quantified using ImageJ software (NIH, Bethesda, MD, USA).

2.4 Protein phosphatase assays

The activity of protein phosphatases 1 (PP1) and 2A (PP2A) was measured with a fluorescence-based assay kit (RediPlate^{TM} EnzChek^{R} serine/threonine phosphatase assay kit, Molecular Probes, USA), according to manufacturer's instructions. Briefly, hearts were homogenized in homogenization buffer containing 150 mM NaCl, 50 mM Tris–HCl, 50 mM NaF, 2% Triton X-100, 0.1% SDS, and 1% (vol/vol) protease inhibitor cocktail (Millipore, Billerica, MA, USA), but no phosphatase inhibitors. For PP1 measurements, 25 μg protein from each sample was diluted in PP1 reaction buffer (optimized with 2 mM DTT and 200 μM $MnCl_2$) to a total volume of 100 μL, and incubated for 30 min in the absence and in the presence of the PP1-specific inhibitor tautomycin (30 nM). For PP2A measurements, 50 μg sample protein was diluted in PP2A reaction buffer (optimized with 1 mM $NiCl_2$) to a total volume of 100 μl, and incubated 30 min with or without the PP2A inhibitor okadaic acid (1 nM). Fluorescence intensity was assayed with a microplate reader using an excitation filter centred at 358 nm and an emission filter at 452 nm. Tautomycin and okadaic acid greatly reduced the fluorescence signal in homogenates from both WT and Ank+/− hearts (see Supplementary material online, *Figure S1*). For each sample, PP1 and PP2A activities were derived by subtracting the fluorescence intensity in the presence of the inhibitor from the signal obtained in its absence.

2.5 Measurement of local Ca^{2+} concentration in the junctional cleft

Local $[Ca^{2+}]_{Cleft}$ was measured using the GCaMP2.2-FKBP12.6 Ca^{2+} sensor as previously described.[17] Isolated mouse cardiomyocytes were plated on laminin-coated cover slips, infected with an adenoviral construct expressing the GCaMP2.2-FKBP12.6 sensor (MOI = 100), and cultured overnight. Membrane staining with Di-8-ANNEPS indicated that mouse myocytes retain the rod shape and the T-tubules network after 24 h in culture (see Supplementary material online, *Figure S2*). GCaMP2.2 fluorescence was recorded with a wide-field fluorescence microscope coupled to a CCD camera (excitation = 490 nm, emission = 540 nm). Two-dimensional images were taken 1 s apart.

2.6 Statistical analysis

Statistical differences between groups were determined using the Student's *t*-test or two-way ANOVA, as appropriate. The data are presented as mean ± standard error. Differences were considered statistically significant when $P < 0.05$. Statistical analysis for single-cell experiments in *Figures 2*, *3*, and *5* were done at the cell level. Data in *Figures 2* and *3* were collected from 3 to 5 myocytes/mouse, while 6–8 cells/mouse were measured for data in *Figure 5*. Since the analysis included a comparable number of myocytes from each mouse, any clustering effects should be minimal.

3. Results

3.1 Ca^{2+} spark frequency is higher in AnkB$^{+/-}$ myocytes due to enhanced CaMKII-dependent phosphorylation of RyRs

We previously demonstrated that RyR gating is altered in myocytes from AnkB$^{+/-}$ mice so that it favours larger Ca^{2+} release events

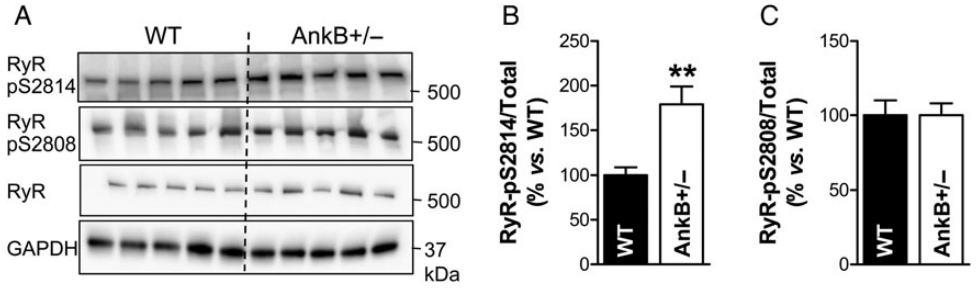

Figure 1 RyR phosphorylation at the CaMKII-specific site is increased in hearts from AnkB$^{+/-}$ mice. (*A*) Representative immunoblots on heart homogenates from WT and AnkB$^{+/-}$ mice using antibodies that recognize RyR phosphorylated at the CaMKII (S2814) and PKA (S2808) sites and total RyR. (*B* and *C*) Ratio of phosphorylated-to-total RyR in hearts from AnkB$^{+/-}$ and WT mice calculated from the relative band intensities. GAPDH was used as loading control. We investigated five hearts/group and immunoblots were repeated four times. Student's *t*-test was used for statistical analysis. $^{**}P < 0.01$.

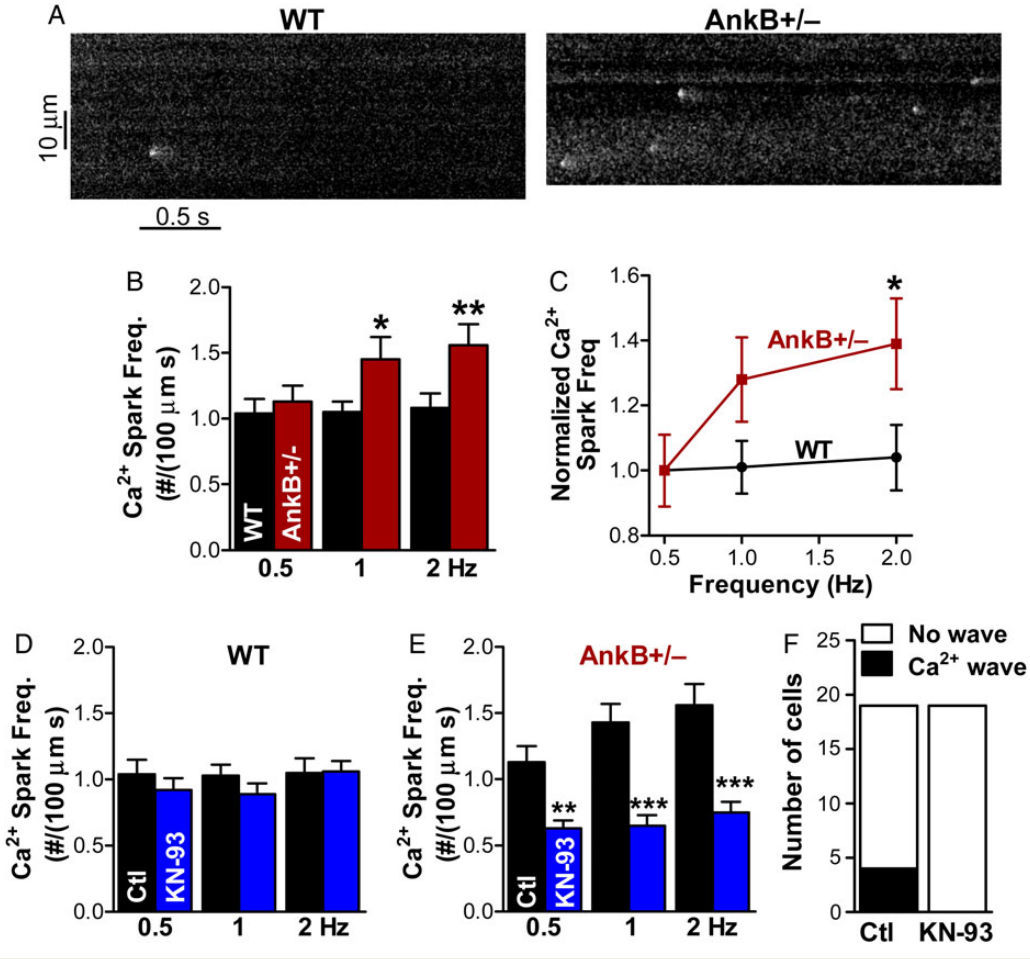

Figure 2 CaMKII inhibition greatly reduces Ca^{2+} spark frequency in AnkB$^{+/-}$ mice. (*A*) Representative Ca^{2+} sparks recordings in myocytes from WT and AnkB$^{+/-}$ mice. Cells were pre-conditioned by steady-state pacing at 1 Hz. (*B*) Mean Ca^{2+} spark frequency in WT and AnkB$^{+/-}$ myocytes pre-conditioned by steady-state pacing at 0.5, 1, and 2 Hz. Data were collected from 17 myocytes (five different mice) for WT and 19 cells (four mice) for AnkB$^{+/-}$. (*C*) Ca^{2+} spark frequency normalized to the mean value in cells pre-conditioned by pacing at 0.5 Hz. (*D* and *E*) Effect of CaMKII inhibition with KN-93 (1 µmol/L) on Ca^{2+} spark frequency in myocytes from WT (*D*) and AnkB$^{+/-}$ (*E*) mice. KN-93 data were collected from 20 myocytes (five mice) for the WT and 19 cells (four mice) for AnkB$^{+/-}$ mice. (*F*) KN-93 suppresses the occurrence of Ca^{2+} waves in AnkB$^{+/-}$ myocytes. In panels *B*–*E*, statistical differences between groups (AnkB$^{+/-}$ vs. WT in panels *B* and *C*, control vs. KN-93 in panels *D* and *E*) were determined using two-way ANOVA with Bonferroni post-test to compare spark frequency for each rate of pre-conditioning pulses. $^{*}P < 0.05$, $^{**}P < 0.01$, and $^{***}P < 0.001$.

(i.e. Ca^{2+} sparks) at the expense of smaller, non-spark releases.[15] Several post-translational modifications of RyRs, including phosphorylation, are known to increase Ca^{2+} spark frequency. Here, we used immunoblot and phospho-specific antibodies to assess the phosphorylation status of RyR at Ser2814 and Ser2808, which are targets for phosphorylation by CaMKII and PKA, respectively (*Figure 1*). We found that RyR phosphorylation at the CaMKII site is enhanced in hearts from AnkB$^{+/-}$ vs. WT mice (*Figure 1A* and *B*; $P = 0.007$), while phosphorylation at the PKA site is similar (*Figure 1A* and *C*; $P = 1.0$). These data agree well with previously published data.[16]

Thus, the higher Ca^{2+} spark frequency in AnkB$^{+/-}$ myocytes may be due to elevated CaMKII-dependent RyR phosphorylation. To test this hypothesis, we measured Ca^{2+} sparks in the absence and in the presence of CaMKII inhibition (*Figure 2*). In these experiments, myocytes from WT and AnkB$^{+/-}$ mice were pre-incubated in Tyrode's solution with or without the CaMKII inhibitor KN-93 (1 μM). After 20 min, cells were superfused with the same solution ($\pm$KN-93) and stimulated at various pacing frequencies (0.5, 1, and 2 Hz) until Ca^{2+} transients reached steady state. Stimulation was then stopped and spontaneous Ca^{2+} sparks were recorded in a $0Na^{+}/0Ca^{2+}$ Tyrode's solution. As in our previous study, the frequency of Ca^{2+} sparks was significantly larger in AnkB$^{+/-}$ myocytes vs. WT (*Figure 2A* and *B*; $P = 0.002$ using two-way ANOVA). Moreover, Ca^{2+} spark frequency raised rather steeply with the rate of pre-conditioning pulses in AnkB$^{+/-}$ myocytes, while it was practically independent of pacing in the WT cells (*Figure 2B* and *C*). This characteristic was maintained after normalizing to the SR Ca^{2+} load (see Supplementary material online, *Figure S3*). This distinct dependence on pre-conditioning may thus be the result of increased diastolic Ca^{2+} accumulation, and consequent RyR activation, with higher pacing rates in AnkB$^{+/-}$ myocytes. The width at half-maximum of Ca^{2+} sparks was higher in AnkB$^{+/-}$ myocytes, while the spark amplitude and duration were similar in cells from AnkB$^{+/-}$ and WT mice (*Figure 3*). Increased spark width with unchanged spark amplitude and duration implies a larger 'spark mass' as a result of an augmented Ca^{2+} flux per release event.

Inhibition of CaMKII with KN-93 greatly decreased Ca^{2+} spark frequency in myocytes from AnkB$^{+/-}$ mice ($P < 0.0001$ using two-way ANOVA) but had little effect in the WT ($P = 0.27$; *Figure 2D* and *E*). KN-92, an inactive derivative of KN-93 that is ineffective at inhibiting CaMKII, did not significantly affect Ca^{2+} spark frequency in AnkB$^{+/-}$ myocytes (see Supplementary material online, *Figure S4*). This result suggests that the effect of KN-93 is mediated specifically by CaMKII inhibition. With CaMKII blocked, Ca^{2+} spark frequency in AnkB$^{+/-}$ myocytes was lower than in WT cells, despite a larger SR Ca^{2+} content (caffeine $\Delta F/F_0 = 9.4 \pm 0.3$ in AnkB$^{+/-}$ vs. 8.4 ± 0.3 in WT myocytes treated with KN-93). It is thus possible that CaMKII inhibition unmasks a secondary mechanism through which AnkB affects RyR function that results in lower Ca^{2+} spark frequency in AnkB$^{+/-}$ myocytes. This is conceivable since RyR activity is regulated by interaction with several proteins and various post-translational modifications, including oxidation, nitrosylation, and glutahionylation. However, the CaMKII-dependent activation of RyR is the prevalent physiological effect of AnkB reduction since Ca^{2+} spark frequency is increased in AnkB$^{+/-}$ myocytes under control conditions.

CaMKII inhibition also abolished the occurrence of Ca^{2+} waves in AnkB$^{+/-}$ myocytes (*Figure 2F*). Combined, the findings in *Figures 1* and *2* suggest that the higher Ca^{2+} spark frequency in AnkB$^{+/-}$ myocytes is due to enhanced RyR phosphorylation by CaMKII.

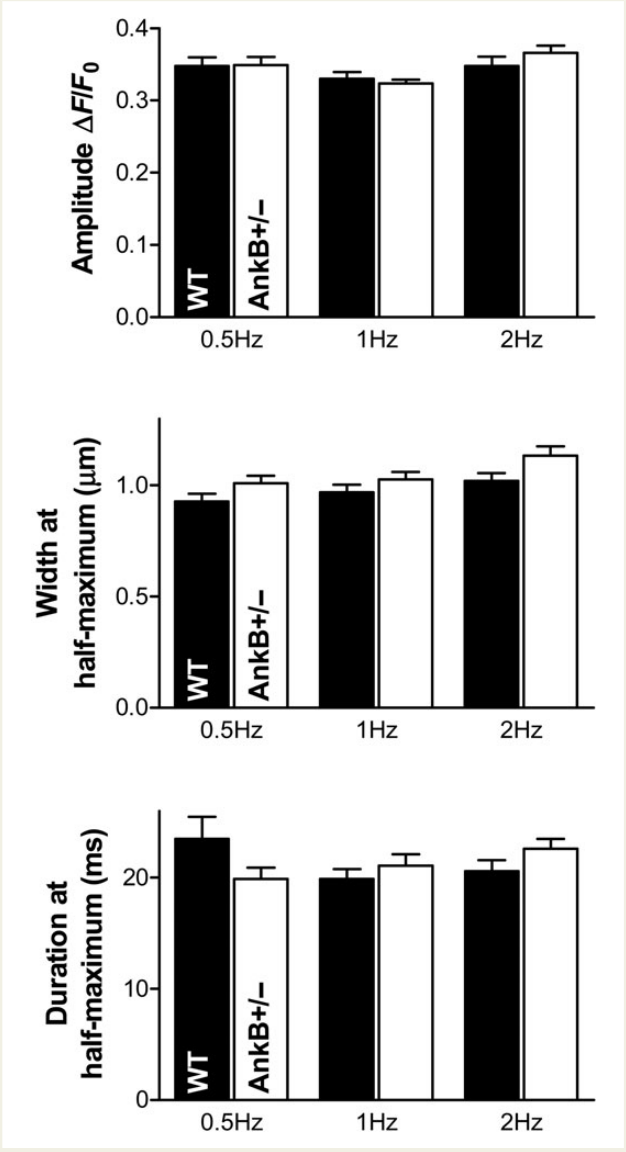

Figure 3 The full width at half-maximum (FWHM) of Ca^{2+} sparks is larger in AnkB$^{+/-}$ myocytes, while spark amplitude and duration are similar in cells from AnkB$^{+/-}$ and WT mice. Statistical analysis was done using the two-way ANOVA test. $P = 0.0067$ for the AnkB-dependence of FWHM. Data are from the same cells as in *Figure 2*.

3.2 CaMKII-mediated protein hyperphosphorylation in AnkB$^{+/-}$ myocytes is a local rather than global effect

Protein phosphorylation is the net result of a delicate balance between the activity of kinases and phosphatases. AnkB is essential for targeting the regulatory subunit B56α of protein phosphatase 2A (PP2A) and B56α localization is altered in AnkB$^{+/-}$ myocytes.[21] Abnormal B56α distribution may modify the PP2A activity and, since PP2A is associated with RyR, may alter RyR phosphorylation. However, we found that the phosphatase activity of PP2A was similar in hearts from AnkB$^{+/-}$ and WT mice (*Figure 4A*; $P = 0.14$). Moreover, the activity of protein phosphatase 1 (PP1), the other phosphatase associated with RyR, was also unaffected in AnkB$^{+/-}$ hearts (*Figure 4A*; $P = 0.72$). While we cannot

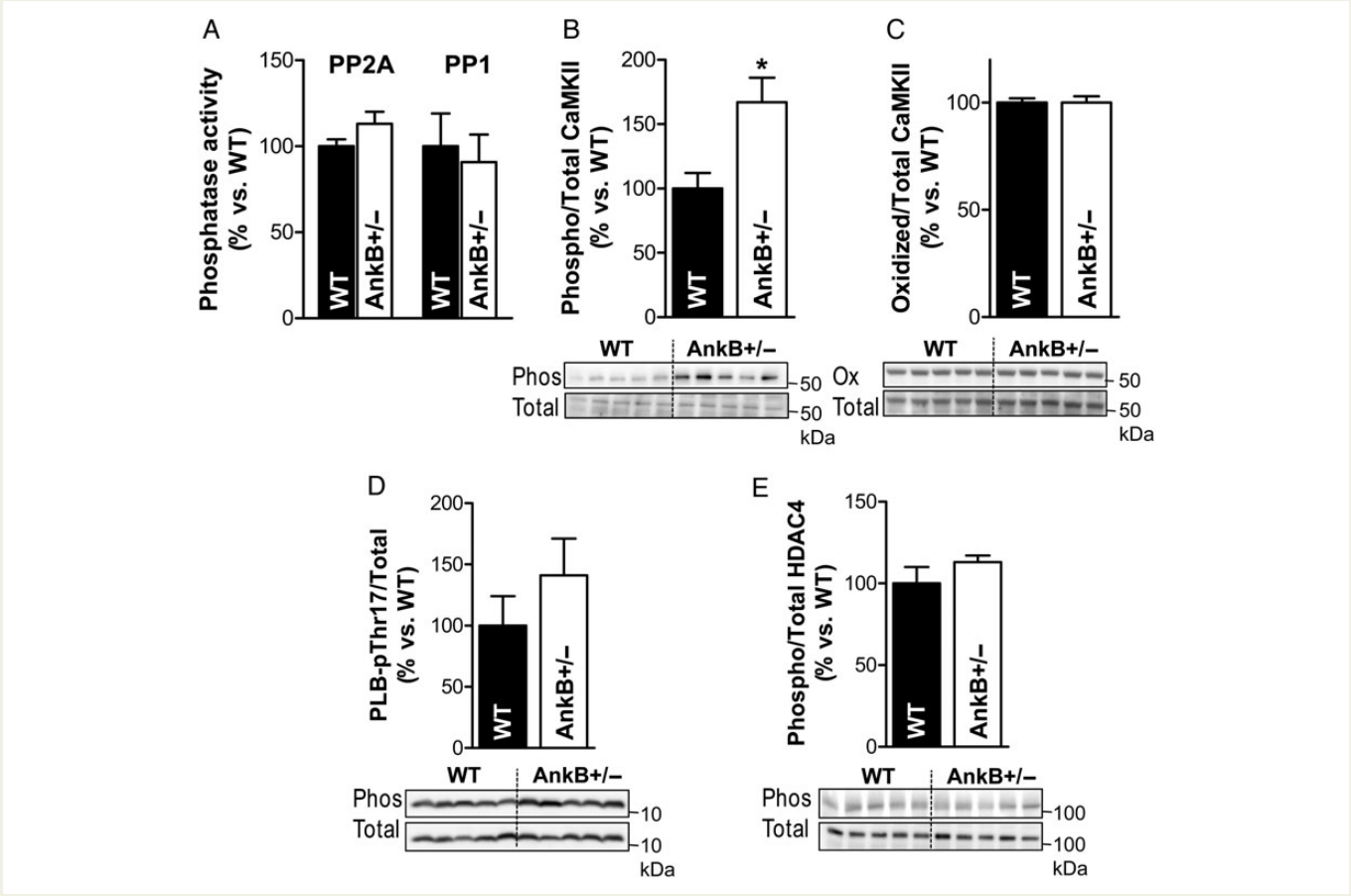

Figure 4 CaMKII activity is increased but CaMKII-mediated phosphorylation of phospholamban and HDAC4 is not modified in AnkB$^{+/-}$ hearts. (*A*) Relative activity of protein phosphatases PP2A and PP1 in hearts from AnkB$^{+/-}$ vs. WT mice. $n = 5$ hearts/group. Experiments were performed in triplicate. (*B*) Ratio of CaMKII autophosphorylated at T287 to total CaMKII from AnkB$^{+/-}$ and WT hearts calculated from the relative band intensities. The bottom panel shows a representative example. $n = 5$ hearts/group, and immunoblots were repeated six times. (*C*) Oxidized-to-total CaMKII in AnkB$^{+/-}$ vs. WT hearts. $n = 5$ hearts/group, and immunoblots repeated four times. (*D*) PLB phosphorylated at Thr17 vs. total PLB in hearts from WT and AnkB$^{+/-}$ mice. $n = 5$ hearts/group, and immunoblots were repeated six times. (*E*) Ratio of phosphorylated-to-total HDAC4 in AnkB$^{+/-}$ and WT hearts. $n = 5$ hearts/group. Experiments were performed in triplicate. Student's *t*-test was used for statistical analysis. $^*P < 0.5$.

exclude the possibility that 'local' activities of PP1 or PP2A are altered, these results indicate that the increased CaMKII-dependent phosphorylation of RyRs in AnkB$^{+/-}$ hearts is not caused by decreased 'global' phosphatase activity. Therefore, we next tested whether the CaMKII activity is increased in AnkB-deficient hearts.

Activation of CaMKII is initiated by the binding of Ca^{2+}/calmodulin, which disrupts the association between the catalytic and regulatory domains of the kinase and exposes the catalytic domain for substrate binding. This conformational change also facilitates post-translational modifications of CaMKII, particularly autophosphorylation at the T287 site and oxidation at M281/M282, that result in autonomous activation of the kinase.[22] We found significantly increased CaMKII phosphorylation at T287 in hearts from AnkB$^{+/-}$ mice (*Figure 4B*; $P = 0.017$), while CaMKII oxidation was similar in AnkB$^{+/-}$ and WT hearts (*Figure 4C*; $P = 1.0$). Thus, CaMKII is activated in AnkB$^{+/-}$ hearts vs. the WT.

To determine whether this increase in CaMKII function is a global effect, we assessed the phosphorylation status of two other well-known CaMKII targets: phospholamban (PLB, at Thr17) and HDAC4 (at Ser632). In contrast to RyRs, the CaMKII-dependent phosphorylation of PLB and HDAC was not significantly enhanced in AnkB$^{+/-}$ hearts (*Figure 4D* and *E*; $P = 0.32$ and 0.26 for PLB and HDAC4, respectively). This result raises the possibility that CaMKII is activated only locally, near RyR, and not within the entire myocyte. Indeed, RyRs are localized mainly in the junctional SR membrane, where the SR comes in very close proximity to sarcolemma,[23–25] whereas PLB and HDAC4 are located away from the junctions.

3.3 Local [Ca^{2+}] in the junctional cleft is elevated in myocytes from AnkB$^{+/-}$ mice

The activity of CaMKII in the junctional cleft could be elevated in myocytes from AnkB$^{+/-}$ mice compared with the WT if local $[Ca^{2+}]_{Cleft}$ is higher in AnkB$^{+/-}$ myocytes. This is conceivable, since AnkB directly associates with NCX,[1–6] and myocytes from AnkB$^{+/-}$ mice show lower levels of NCX, particularly at the T-tubules, where the junctions are mainly located.[1] A reduction in junctionally localized NCX slows down Ca^{2+} extrusion from the cleft and may result in elevated $[Ca^{2+}]_{Cleft}$ (see cartoon in *Figure 5A*). This hypothesis is supported by prior studies demonstrating that NCX inhibition results in increased Ca^{2+} spark frequency without significant changes in the SR Ca^{2+} content.[26,27]

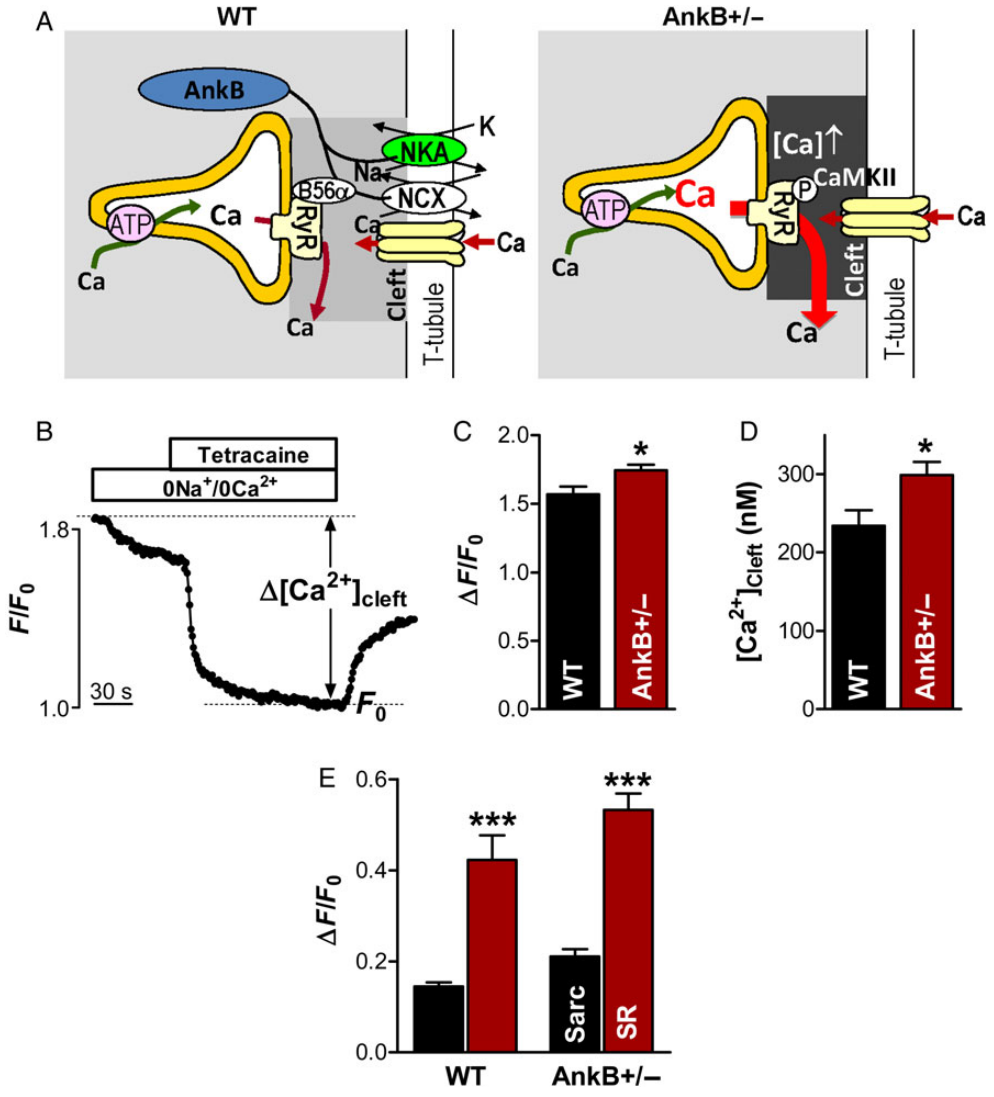

Figure 5 $[Ca^{2+}]_{Cleft}$ is increased in myocytes from $AnkB^{+/-}$ mice. (*A*) Working hypothesis. NCX and NKA density in the T-tubules is reduced in myocytes from $AnkB^{+/-}$ mice, which may result in slower Ca^{2+} extrusion from the junctional cleft and consequently elevated $[Ca^{2+}]_{Cleft}$ compared with WT myocytes. This higher $[Ca^{2+}]_{Cleft}$ may activate RyR through direct sensitization and indirectly by activating local CaMKII. (*B*) Example of $[Ca^{2+}]_{Cleft}$ measurements with GCaMP2.2-FKBP12.6. (*C*) Mean decrease in fluorescence intensity upon application of $0Na^{+}/0Ca^{2+}$ external solution and tetracaine for $AnkB^{+/-}$ and WT myocytes. (*D*) $[Ca^{2+}]_{Cleft}$ calculated from data in panel *C* using the *in situ* characteristics of GCaMP2.2-FKBP12.6. (*E*) Mean decrease in GCaMP2.2-FKBP12.6 fluorescence upon inhibition of sarcolemmal Ca^{2+} transport in $0Na^{+}/0Ca^{2+}$ solution (Sarc) and blockade of SR Ca^{2+} leak with tetracaine (SR). Data in panels *C*–*E* are from 24 cells from three different $AnkB^{+/-}$ mice and 20 cells from three WT mice. Statistical differences between groups were determined using Student's *t*-test. $*P < 0.05$ and $***P < 0.001$.

We tested this hypothesis by measuring the diastolic $[Ca^{2+}]_{Cleft}$ in $AnkB^{+/-}$ and WT myocytes using our newly developed GCaMP2.2-FKBP12.6 $[Ca^{2+}]_{Cleft}$ sensor.[17] The sensor was created by attaching the genetically encoded Ca^{2+} sensor GCaMP2.2 to FKBP12.6, a protein that binds with high affinity and specificity to RyR monomers, but does not greatly influence RyR function.[28] GCaMP2.2-FKBP12.6 was expressed in intact myocytes by adenoviral infection and cells were used for experiments 20–24 h later. We previously demonstrated rigorously that expressed this way, the sensor reports local $[Ca^{2+}]_{Cleft}$.[17] To measure diastolic $[Ca^{2+}]_{Cleft}$, myocytes were first field-stimulated (at 0.5 Hz) to reach steady state. Then stimulation was stopped and we blocked Ca^{2+} fluxes into the cleft by switching to a $0Na^{+}/0Ca^{2+}$ external solution, which prevents Ca^{2+} movement through both L-type Ca^{2+} channels and NCX, followed by application of 1 mM tetracaine, a RyR inhibitor (*Figure 5B*). Under these conditions, $[Ca^{2+}]_{Cleft}$ declines, and in the new steady state (F_0), any $[Ca^{2+}]$ gradient between the cleft and bulk cytosol dissipates.[17] Since diastolic $[Ca^{2+}]_i$ in the bulk cytosol is similar in $AnkB^{+/-}$ and WT myocytes (85 ± 6 vs. 87 ± 5 nM, measured by us[15]), at the F_0 steady state, the sensor detects the same Ca^{2+} concentration in WT and AnkB-deficient myocytes. Therefore, the F_0 state was used to normalize the GCaMP-FKBP12.6 fluorescence intensity in different cells (*Figure 5B*). The decrease in GCaMP2.2-FKBP12.6 fluorescence induced by inhibition of Ca^{2+} fluxes into the cleft was significantly greater in myocytes from $AnkB^{+/-}$ mice compared with the WT (*Figure 5C*; $P = 0.014$), which indicates that $[Ca^{2+}]_{Cleft}$ is higher in the $AnkB^{+/-}$

myocytes. Using the *in situ* GCaMP2.2-FKBP12.6 characteristics that we previously measured[17] ($F_{max}/F_{min} = 6$, $K_d = 1100$ nM, and $n_{Hill} = 1$), we calculated that $[Ca^{2+}]_{Cleft}$ is 299 ± 17 nM in $AnkB^{+/-}$ myocytes and 234 ± 20 nM in WT cells (*Figure 5D*; $P = 0.017$). Thus, AnkB deficiency leads to a local increase of diastolic [Ca^{2+}] in the junctional cleft.

For both WT and $AnkB^{+/-}$ myocytes, the decrease in GCaMP2.2-FKBP12.6 signal was significantly greater upon inhibition of the SR Ca^{2+} leak compared with the blockade of sarcolemmal Ca^{2+} fluxes (*Figure 5B* and *E*; $P < 0.0001$). This means that SR Ca^{2+} leak rather than Ca^{2+} entry across sarcolemma is the main source of Ca^{2+} in the junctional cleft in myocytes from WT and $AnkB^{+/-}$ mice, similar to what we previously found in rat myocytes.[17]

4. Discussion

We previously found that reduced AnkB function modifies the RyR gating so that a larger fraction of the SR Ca^{2+} leak occurs through Ca^{2+} sparks.[15] These more coordinated RyRs openings result in a higher propensity for Ca^{2+} waves,[15,29] which may contribute to the increased arrhythmogenicity in AnkB-deficient hearts. Here, we found that the increased frequency of Ca^{2+} sparks and waves in $AnkB^{+/-}$ myocytes is due to enhanced phosphorylation of RyRs by CaMKII. This result agrees well with prior observations that CaMKII inhibition normalizes the RyR open probability and rescues the abnormal electrical activity in $AnkB^{+/-}$ hearts.[16] We further demonstrated that the CaMKII-dependent RyR hyperphosphorylation is caused by augmented CaMKII activity rather than reduced function of protein phosphatases. Intriguingly, CaMKII activation seems to be limited to the junctional space where the sarcolemma and SR membrane come in close proximity since CaMKII targets located outside the junctions (phospholamban and HDAC4) are not hyperphosphorylated in $AnkB^{+/-}$ myocytes. The activity of junctionally located CaMKII is likely increased in AnkB-deficient hearts by a higher local [Ca^{2+}] in the cleft. Indeed, we found that although the global diastolic $[Ca^{2+}]_i$ is similar in myocytes from $AnkB^{+/-}$ and WT mice, the local $[Ca^{2+}]_{Cleft}$ is significantly elevated in $AnkB^{+/-}$ myocytes.

A prior study[16] reported enhanced RyR phosphorylation at the CaMKII site in myocytes from $AnkB^{+/-}$ mice. However, the cause for this increase (higher CaMKII activity vs. reduced phosphatase function) was not previously determined. AnkB binds to and targets the regulatory subunit B56α of PP2A,[21] which raises the possibility that PP2A activity is altered in $AnkB^{+/-}$ myocytes. However, we found similar PP2A function in WT and AnkB-deficient myocytes. The B56α subunit was recently shown to have an autoinhibitory role that suppresses PP2A activity, so that lower B56α levels resulted in fewer Ca^{2+} waves and sparks and decreased RyR phosphorylation.[30] This further supports our conclusion that the RyR hyperphosphorylation in $AnkB^{+/-}$ myocytes is due to increased CaMKII activity rather than lower phosphatase activity.

$[Ca^{2+}]_i$ is regulated and signals differently in various subcellular microdomains, which greatly enhances its versatility as a secondary messenger.[31–32] In the heart, the SR Ca^{2+} release is controlled locally by the [Ca^{2+}] in the restricted space between the sarcolemma and junctional SR. It is increasingly recognized that $[Ca^{2+}]_{Cleft}$ is regulated differently from the bulk $[Ca^{2+}]_i$, both during electrical excitation and at rest.[17–19,24,33] While the mechanisms leading to higher $[Ca^{2+}]_{Cleft}$ in AnkB-deficient myocytes compared with WT are not fully elucidated, we hypothesize that the reduced expression and altered localization of NCX is a major player. AnkB directly associates with NCX,[1–6] and AnkB mutants that lose the ability to target NCX to the membrane result in congenital arrhythmias.[1,3] Cardiac myocytes from $AnkB^{+/-}$ mice show drastically reduced NCX localization at the T-tubules.[1] In control myocytes, ~25% of the T-tubular NCX is co-localized with RyR at the junctions.[25] During diastole, Ca^{2+} removal by the junctionally located NCX keeps local $[Ca^{2+}]_{Cleft}$ low (*Figure 5A*) and limits Ca^{2+} release within a given RyRs cluster.[34] Reduced NCX expression in $AnkB^{+/-}$ myocytes slows down Ca^{2+} extrusion from the cleft, which may result in elevated $[Ca^{2+}]_{Cleft}$ and therefore enhanced spark-mediated SR Ca^{2+} release. Studies showing that NCX inhibition leads to increased Ca^{2+} spark frequency in the absence of significant changes in the SR Ca^{2+} content[26,27] support this hypothesis. Moreover, functional evidence (reduced availability of L-type Ca^{2+} channels and enhanced ability of the non-inactivated channels to trigger SR Ca^{2+} release) indicates that $[Ca^{2+}]_{Cleft}$ is elevated in myocytes from cardiac-specific NCX knockout mice.[35] Besides activating local CaMKII and consequently increasing the CaMKII-mediated RyR phosphorylation, elevated $[Ca^{2+}]_{Cleft}$ may also promote the occurrence of Ca^{2+} sparks and waves through direct RyR sensitization.

In summary, we found that the higher incidence of pro-arrhythmogenic Ca^{2+} sparks and waves in AnkB-deficient myocytes is due to enhanced phosphorylation of RyRs by CaMKII. This CaMKII-dependent RyR hyperphosphorylation is the result of activation of CaMKII located at the sarcolemma–SR junctions by an elevated [Ca^{2+}] in the junctional cleft.

Supplementary material

Supplementary material is available at *Cardiovascular Research* online.

Acknowledgements

The authors thank Drs Donald M. Bers and Julie Bossuyt from University of California Davis for constructing and multiplying the GCaMP2.2-FKBP12.6 Ca^{2+} sensor.

Conflict of interest: none declared.

Funding

This work was supported by the National Institutes of Health (grants HL109501 to S.D. and HL084583 to P.J.M.).

References

1. Mohler PJ, Schott JJ, Gramolini AO, Dilly KW, Guatimosin S, duBell WH, Song LS, Haurogne K, Kyndt F, Ali ME, Rogers TB, Lederer WJ, Escande D, Le Marec H, Bennett V. Ankyrin-B mutation causes type 4 long-QT cardiac arrhythmia and sudden cardiac death. *Nature* 2003;**421**:634–639.
2. Mohler PJ, Splawski I, Napolitano C, Bottelli G, Sharpe L, Timothy K, Priori SG, Keating MT, Benett V. A cardiac arrhythmia syndrome caused by loss of ankyrin-B function. *Proc Natl Acad Sci USA* 2004;**101**:9137–9142.
3. Mohler PJ, Le Scouarnec S, Denjoy I, Lowe JS, Guicheney P, Caron L, Driskell IM, Schott JJ, Norris K, Leenhardt A, Kim RB, Escande D, Roden DM. Defining the cellular phenotype of 'ankyrin-B syndrome' variants: human ANK2 variants associated with clinical phenotypes display a spectrum of activities in cardiomyocytes. *Circulation* 2007;**115**:432–441.
4. Li Z, Burke EP, Frank JS, Bennett V, Philipson KD. The cardiac Na^+-Ca^{2+} exchanger binds to the cytoskeletal protein ankyrin. *J Biol Chem* 1992;**117**:337–345.
5. Cunha SR, Bhasin N, Mohler PJ. Targeting and stability of Na/Ca exchanger 1 in cardiomyocytes requires direct interaction with the membrane adaptor ankyrin-B. *J Biol Chem* 2007;**282**:4875–4883.
6. Mohler PJ, Davis JQ, Bennet V. Ankyrin-B coordinates the Na/K ATPase, Na/Ca exchanger, and InsP3 receptor in a cardiac T-tubule/SR microdomain. *PLoS Biol* 2005;**3**:e423.
7. Devarajan P, Scaramuzzino DA, Morrow JS. Ankyrin binds to two distinct cytoplasmic domains of Na,K-ATPase α subunit. *Proc Natl Acad Sci USA* 1994;**91**:2965–2969.

8. Smith SA, Sturm AC, Curran J, Kline CF, Little SC, Bonilla IM, Long VP, Makara M, Polina I, Hughes LD, Webb TR, Wei Z, Wright P, Voigt N, Bhakta D, Spoonamore KG, Zhang C, Weiss R, Binkley PF, Janssen PM, Kilic A, Higgins RS, Sun M, Ma J, Dobrev D, Zhang M, Carnes CA, Vatta M, Rasband MN, Hund TJ, Mohler PJ. Dysfunction in the βII spectrin-dependent cytoskeleton underlies human arrhythmia. *Circulation* 2015;**131**:695–708.
9. Le Scouarnec S, Bhasin N, Vieyres C, Hund TJ, Cunha SR, Koval O, Marionneau C, Chen B, Wu Y, Demolombe S, Song LS, Le Marec H, Probst V, Schott JJ, Anderson ME, Mohler PJ. Dysfunction in ankyrin-B-dependent ion channel and transporter targeting causes human sinus node disease. *Proc Natl Acad Sci USA* 2008;**105**:15617–15622.
10. Cunha SR, Hund TJ, Hashemi S, Voigt N, Li N, Wright P, Koval O, Li J, Gudmundsson H, Gumina RJ, Karck M, Schott JJ, Probst V, Le Marec H, Anderson ME, Dobrev D, Wehrens XH, Mohler PJ. Defects in ankyrin-based membrane protein targeting pathways underlie atrial fibrillation. *Circulation* 2011;**124**:1212–1222.
11. Bers DM. Cardiac sarcoplasmic reticulum calcium leak: basis and roles in cardiac dysfunction. *Annu Rev Physiol* 2014;**76**:107–127.
12. Santiago DJ, Curran JW, Bers DM, Lederer WJ, Stern MD, Rios E, Shannon TR. Ca sparks do not explain all ryanodine receptor-mediated SR Ca leak in mouse ventricular myocytes. *Biophys J* 2010;**98**:2111–e420.
13. Zima AV, Bovo E, Bers DM, Blatter LA. Ca^{2+} spark-dependent and -independent sarcoplasmic reticulum Ca^{2+} leak in normal and failing rabbit ventricular myocytes. *J Physiol* 2010;**588**:4743–4757.
14. Brochet DX, Xie W, Yang D, Cheng H, Lederer WJ. Quarky calcium release in the heart. *Circ Res* 2011;**108**:210–218.
15. Camors E, Mohler PJ, Bers DM, Despa S. Ankyrin-B reduction alters Na and Ca transport promoting cardiac myocyte arrhythmic activity. *J Mol Cell Cardiol* 2012;**52**:1240–1248.
16. DeGrande S, Nixon D, Koval O, Curran JW, Wright P, Wang Q, Kashef F, Chiang D, Li N, Wehrens XH, Anderson ME, Hund TJ, Mohler PJ. CaMKII inhibition rescues proarrhythmic phenotypes in the model of human ankyrin-B syndrome. *Heart Rhythm* 2012;**9**:2034–2041.
17. Despa S, Shui B, Bossuyt J, Lang D, Kotlikoff MI, Bers DM. Junctional cleft $[Ca^{2?}]_i$ measurements using novel cleft-targeted $Ca^{2?}$ sensors. *Circ Res* 2014;**115**:339–347.
18. Acsai K, Antoons G, Livshitz L, Rudy Y, Sipido KR. Microdomain $[Ca^{2+}]$ near ryanodine receptors as reported by L-type Ca^{2+} and Na^+/Ca^{2+} exchange currents. *J Physiol* 2011;**589**:2569–2583.
19. Shang W, Lu F, Sun T, Xu J, Li LL, Wang Y, Wang G, Chen L, Wang X, Cannell MB, Wang SQ, Cheng H. Imaging Ca^{2+} nanosparks in heart with a new targeted biosensor. *Circ Res* 2014;**114**:412–420.
20. Picht E, Zima AV, Blatter LA, Bers DM. SparkMaster: automated calcium spark analysis with ImageJ. *Am J Physiol Cell Physiol* 2007;**293**:C1073–C1081.
21. Bhasin N, Cunha SR, Mudannayake M, Gigena MS, Rogers TB, Mohler PJ. Molecular basis for PP2A regulatory subunit B56α targeting in cardiomyocytes. *Am J Physiol Heart Circ Physiol* 2007;**293**:H109–H119.
22. Erickson JR. Mechanisms of CaMKII activation in the heart. *Front Pharmacol* 2014;**2**:59.
23. Bers DM. *Excitation-Contraction Coupling and Cardiac Contractile Force*. 2nd ed. Dordrecht, Boston, London: Kluwer Academic Publishers; 2001.
24. Guatimosim S, Dilly K, Santana LF, Saleet Jafri M, Sobie EA, Lederer WJ. Local Ca^{2+} signaling and EC coupling in heart: Ca^{2+} sparks and the regulation of the $[Ca^{2+}]_i$ transient. *J Mol Cell Cardiol* 2002;**34**:941–950.
25. Jayasinghe ID, Cannell MB, Soeller C. Organization of ryanodine receptors, transverse tubules, and sodium-calcium exchanger in rat myocytes. *Biophys J* 2009;**97**:2664–2673.
26. Goldhaber JI, Lamp ST, Walter DO, Garfinkel A, Fukumoto GH, Weiss JN. Local regulation of the threshold for calcium sparks in rat ventricular myocytes: role of sodium-calcium exchange. *J Physiol* 1999;**520**:431–438.
27. Bovo E, de Tombe PP, Zima AV. The role of dyadic organization in regulation of sarcoplasmic reticulum Ca^{2+} handling during rest in rabbit ventricular myocytes. *Biophys J* 2014;**106**:1902–1909.
28. Guo T, Cornea RL, Huke S, Camors E, Yang Y, Picht E, Fruen BR, Bers DM. Kinetics of FKBP12.6 binding to ryanodine receptors in permeabilized cardiac myocytes and effects on Ca sparks. *Circ Res* 2010;**106**:1743–1752.
29. Stokke MK, Tovsrud N, Louch WE, Øyehaug L, Hougen K, Sejersted OM, Swift F, Sjaastad I. I_{CaL} inhibition prevents arrhythmogenic Ca^{2+} waves caused by abnormal Ca^{2+} sensitivity of RyR or SR Ca^{2+} accumulation. *Cardiovasc Res* 2013;**98**:315–325.
30. Little SC, Curran J, Makara MA, Kline CF, Ho HT, Xu Z, Wu X, Polina I, Musa H, Meadows AM, Carnes CA, Biesiadecki BJ, Davis JP, Weisleder N, Györke S, Wehrens XH, Hund TJ, Mohler PJ. Protein phosphatase 2A regulatory subunit B56α limits phosphatase activity in the heart. *Sci Signal* 2015;**8**:ra72.
31. Parekh AB. Ca^{2+} microdomains near plasma membrane Ca^{2+} channels: impact on cell function. *J Physiol* 2008;**586**:3043–3054.
32. Berridge MJ. Calcium microdomains: organization and function. *Cell Calcium* 2006;**40**:405–412.
33. Sipido KR, Callewaert G, Carmeliet E. Inhibition and rapid recovery of ICa during calcium release from the sarcoplasmic reticulum in guinea-pig ventricular myocytes. *Circ Res* 1995;**76**:102–109.
34. Sato D, Despa S, Bers DM. Can the sodium-calcium exchanger initiate or suppress calcium sparks in cardiac myocytes? *Biophys J* 2012;**102**:L31–L33.
35. Pott C, Yip M, Goldhaber JI, Philipson KD. Regulation of cardiac L-type Ca^{2+} current in Na^+-Ca^{2+} exchanger knockout mice: functional coupling of the Ca^{2+} channel and the Na^+-Ca^{2+} exchanger. *Biophys J* 2007;**92**:1431–1437.